

On the scattering of evanescent waves into sound

By J. E. FFOWCS WILLIAMS AND D. C. HILL

Cambridge University Engineering Department, Trumpington Street,
Cambridge CB2 1PZ, UK

(Received 27 March 1986 and in revised form 24 March 1987)

This paper concerns the conversion of momentum and energy from evanescent surface waves into sound. Exact results are obtained from surface waves of specified form on a confined region of an otherwise rigid plane surface. The model chosen is simple enough for exact analysis while approximating some of what we believe to be significant aspects of sound generation by vibrating surface panels.

We find that the evanescent wave approaching an edge gives up all of its energy into sound, a sound which is beamed mainly parallel to the direction of the surface-wave phase velocity. The surface remains energetically inactive, but exerts a force on the fluid in the opposite direction to the incoming wave. This force is balanced by a nonlinear mean pressure gradient in the field of the evanescent wave, and by momentum in the sound field.

Sound is also produced when a similar evanescent wave emerges from an edge. The surface has then to provide the necessary energy for both waves. These waves induce a mean axial force at the boundary which forces the fluid in the direction of the receding evanescent wave.

A similar wave travelling across a finite panel in the otherwise rigid plane surface is observed to have some characteristics of the previous two cases, but there is no axial force arising from the mean pressure gradient.

These results are applied to the problem of a semi-infinite tensioned membrane, and the energy radiation under light fluid loading is determined for the case of high and low free membrane wave speeds.

1. Introduction

Surface waves with subsonic phase velocity are evanescent and only weakly affected by the fluid's compressibility. But any interruption of the wave system causes some of the surface wave's energy to be scattered into sound, the degree of the conversion process obviously depending on the precise nature of the scatterer. One extreme of the process involves a complete energy conversion. Taylor (1942) showed that impulsively arrested slow flows must evolve into sound waves. Hill (1986) has extended those ideas to an impulsively started evanescent wave, again demonstrating an equipartition of wave energy. In this paper we examine the influence of a different kind of abrupt change, imposing the discontinuity on the spacial rather than the temporal extent of the evanescent field. We find a similar equipartition of energy between the hydrodynamic and acoustic fields. The interest in the problem arises because it throws light on the mechanism by which bounded surface waves generate sound.

Details of wave reflection and scattering at the edge of a vibrating panel are very involved even for surfaces with ideally specified flexural characteristics and

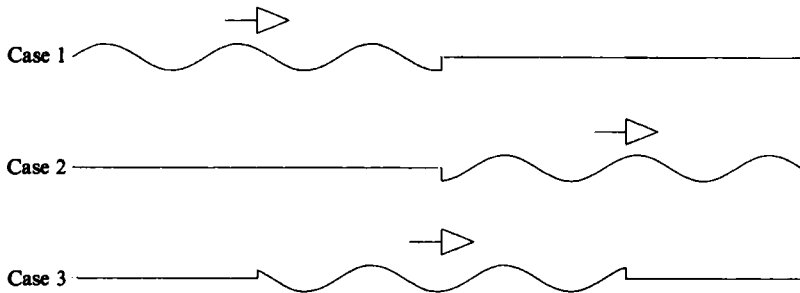


FIGURE 1. Diagram representing the three cases studied.

unrealistically simple edge constraints. The flexural surface motion driven by the intricate edge-scattered pressure field is itself very intricate. Even the ideal problems are hard to analyse because of the need to take account of this mutual cause and effect. And even when the solutions to the few tractable cases are available it is hardly ever straightforward to determine the energy and momentum balance which characterize their acoustic and drag-producing properties. What we present in this paper is a different kind of simplification in which we avoid the issue of how the surface wave is modified by the surface pressure. Then we have a much easier problem whose solution can be interrogated to a greater depth than in the conventional case in which the surface dynamical properties are specified. In fact the solution to the exact problem is almost trivially easy to write down. Even so it is still quite hard to display that solution in sufficient detail to illustrate clearly how sound is generated from a surface wave, where the energy comes from and what force is implied by the scattering process. It is this illustration and the interpretation of the solution that we regard as novel and potentially instructive to others.

We examine three particular cases where an infinite plane surface, bounded on one side by an inviscid fluid, supports harmonic waves of specified amplitude. Some parts of the boundary plane are in prescribed motion; elsewhere the surface is undisturbed. The junction between the moving and still parts is the cause of the wave scattering whose properties we determine in detail.

Our first problem concerns a semi-infinite, subsonic, plane wave travelling towards an edge beyond which the surface is flat. In the second example the wave is driven away from the edge, while the third concerns waves in a strip of finite width (see figure 1).

In each case we show how the evanescent wave attached to the surface is coupled to cylindrical outwardly travelling sound waves which are centred on each edge.

In studying the energy and momentum flow through the system, care is taken that these quantities are adequately defined. Möhring (1982) has outlined the various approaches possible, and that taken here acknowledges the nonlinearity of the full equations of motion.

We find that when an evanescent wave of fixed amplitude approaches an edge the energy travelling with the wave is transformed by the edge into sound. The surface at large plays a purely passive role in scattering the evanescent disturbance. The surface does no work on the fluid, nor is any work done by the fluid on it. We find that there is a mean form drag on the surface. The surface in turn exerts a mean force on the fluid, a force that acts in the opposite direction to the incoming evanescent

wave. We show that a combination of the flow of momentum through the system, and second-order components of the mean pressure, balance this surface force and maintain the equilibrium of the steady state.

For the second case where waves move away from the edge a totally different energy balance is struck despite the pressure field having a similar form. In this case the surface is active and gives off energy at a rate sufficient to maintain both the evanescent and the sound fields. In contrast to the first case, there is now a force acting at the surface on the fluid in the direction that the evanescent wave is travelling.

Finally, the third case of a wave between two baffles combines both of these effects; there is a 'starting' and a 'stopping' edge. The wavy region acts as a source radiating sound to infinity, its efficiency depending upon the surface wave speed, and the number of wavelengths present in the strip. As the strip is widened, the wave field becomes a superposition of the two previous cases, and twice the acoustic energy is emitted corresponding to the presence of two remotely coupled edges.

The drag on the surface behaves in a similar manner. As the width of the strip becomes large the drag limits to the sum of that due to isolated 'starting' and 'stopping' edges.

In our final section, these results are used to determine characteristics of a semi-infinite fluid-loaded membrane. These agree with those calculated by Davies (1974), who dealt with a tensioned membrane in the light-fluid-loading case using a Wiener-Hopf technique. We give also an estimate of the behaviour when the membrane free wave speed is very high, in which case the conversion of near-field energy into sound is much more efficient.

2. A surface wave approaching an edge

2.1. The pressure field

The outgoing linear pressure field produced by the motion of an infinite plane boundary is given by

$$p(\mathbf{x}, t) = \frac{\rho_0}{2\pi} \int_s \left[\frac{\partial v_n}{\partial t} \right] \frac{dS'}{r}, \quad (2.1)$$

as shown by Hill (1986). For this problem the mean position of the surface is taken to lie in the plane $y = 0$, with the fluid occupying the region $y > 0$.

In order to describe a wave incident on an edge a normal velocity,

$$v_n = vH(-x') e^{i(\omega t - kx')}, \quad \frac{\omega}{k} < c, \quad (2.2)$$

is prescribed. Thus

$$p(\mathbf{x}, t) = i \frac{\rho_0 v \omega}{2\pi} \int_s H(-x') e^{i(\omega t - kx')} \frac{e^{-i\omega r/c}}{r} dS'. \quad (2.3)$$

Integration over the z' variable produces a Hankel function, so that

$$p(\mathbf{x}, t) = \frac{1}{2} \rho_0 v \omega \int_{-\infty}^0 e^{i(\omega t - kx')} H_0^{(2)} \left(\frac{\omega}{c} \left((x - x')^2 + y^2 \right)^{\frac{1}{2}} \right) dx'. \quad (2.4)$$

a result that might have been the alternative starting point of this analysis using the two-dimensional Green function of the Helmholtz equation.

If the integration range in (2.4) were infinite, then the pressure field would be the evanescent wave

$$E(\mathbf{x}, t) = \rho_0 v c \frac{m}{(1 - m^2)^{\frac{1}{2}}} i e^{i(\omega t - kx)} e^{-ky(1 - m^2)^{\frac{1}{2}}}, \tag{2.5}$$

where $m = \omega/kc$. Equation (2.4) can be expressed as

$$p(\mathbf{x}, t) = H(-x) \{E(\mathbf{x}, t) + \frac{1}{2} \rho_0 v \omega C(\mathbf{x}) e^{i\omega t}\} + H(x) \frac{1}{2} \rho_0 v \omega C(\mathbf{x}) e^{i\omega t}, \tag{2.6}$$

where
$$C(\mathbf{x}) = - \int_0^\infty e^{-ikx'} H_0^{(2)} \left(\frac{\omega}{c} ((x-x')^2 + y^2)^{\frac{1}{2}} \right) dx' \quad (x < 0), \tag{2.7}$$

$$= \int_{-\infty}^0 e^{-ikx'} H_0^{(2)} \left(\frac{\omega}{c} ((x-x')^2 + y^2)^{\frac{1}{2}} \right) dx' \quad (x > 0). \tag{2.8}$$

In order to find the structure of C that supplements the evanescent field, the Hankel function is expanded using the ‘Summation Theorem’ stated in Gradshteyn & Ryzhik (1980, p. 979, §8.531).

Then for $x < 0$ (similarly for $x > 0$)

$$H_0^{(2)} \left(\frac{\omega}{c} ((x-x')^2 + y^2)^{\frac{1}{2}} \right) = J_0 \left(\frac{\omega}{c} x' \right) H_0^{(2)} \left(\frac{\omega}{c} r \right) + 2 \sum_{n=1}^\infty J_n \left(\frac{\omega}{c} x' \right) H_n^{(2)} \left(\frac{\omega}{c} r \right) \cos n\theta, \tag{2.9}$$

where $r = (x^2 + y^2)^{\frac{1}{2}}$, and $\theta \in [\frac{1}{2}\pi, \pi]$.

Noting that

$$\int_0^\infty J_n \left(\frac{\omega}{c} x' \right) e^{-ikx'} dx' = - \frac{1}{k} \frac{1}{(1 - m^2)^{\frac{1}{2}}} \frac{m^n}{(1 + (1 - m^2)^{\frac{1}{2}})^n} i e^{-in\frac{1}{2}\pi}, \tag{2.10}$$

and that

$$x = r \cos \theta, \quad y = r \sin \theta, \tag{2.11}$$

then for $\theta \in [0, \pi]$

$$C(r, \theta) = \frac{i}{k} \frac{1}{(1 - m^2)^{\frac{1}{2}}} \left\{ H_0^{(2)} \left(\frac{\omega}{c} r \right) + 2 \sum_{n=1}^\infty \frac{m^n e^{-in\frac{1}{2}\pi}}{(1 + (1 - m^2)^{\frac{1}{2}})^n} H_n^{(2)} \left(\frac{\omega}{c} r \right) \cos n\theta \right\}. \tag{2.12}$$

To find the far-field (large- r) approximation to

$$p(\mathbf{x}, t) = H(-x) E(\mathbf{x}, t) + \frac{1}{2} \rho_0 \omega C(r, \theta) e^{i\omega t} \tag{2.13}$$

the asymptotic form for $H_n^{(2)}$ can be substituted in (2.12):

$$H_n^{(2)}(z) \sim \left(\frac{2}{\pi} \right)^{\frac{1}{2}} \frac{1}{z^{\frac{1}{2}}} e^{-i(z - \frac{1}{4}\pi)} e^{in\frac{1}{2}\pi}. \tag{2.14}$$

Then

$$C(r, \theta) \underset{r \rightarrow \infty}{\sim} \frac{i}{k} \left(\frac{2c}{\pi \omega} \right)^{\frac{1}{2}} \frac{1}{r^{\frac{1}{2}}} e^{i(\frac{1}{4}\pi - \omega r/c)} \frac{1}{(1 - m^2)^{\frac{1}{2}}} \left\{ 1 + 2 \sum_{n=1}^\infty \frac{m^n \cos n\theta}{(1 + (1 - m^2)^{\frac{1}{2}})^n} \right\}. \tag{2.15}$$

The infinite series is convergent, and since (Gradshteyn & Ryzhik 1980, §1.447(2), p. 40)

$$\frac{1}{(1 - m^2)^{\frac{1}{2}}} + \frac{2}{(1 - m^2)^{\frac{1}{2}}} \sum_{n=1}^\infty \frac{m^n \cos n\theta}{(1 + (1 - m^2)^{\frac{1}{2}})^n} = \frac{1}{1 - m \cos \theta}, \tag{2.16}$$

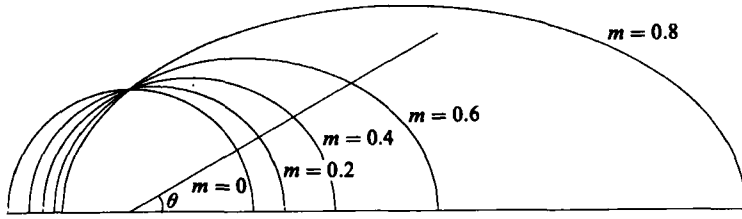


FIGURE 2. The directional dependence of the cylindrical wave amplitude in the form of a polar diagram.

the far field of (2.13) gives

$$p(x, t) \underset{r \rightarrow \infty}{\sim} H(-x) E(x, t) + \frac{A}{r^{\frac{1}{2}}} \frac{1}{1 - m \cos \theta} i e^{i\omega(t-r/c)} e^{i\frac{1}{2}\pi}, \tag{2.17}$$

where
$$A = \frac{\rho_0 v \omega}{k} \left(\frac{c}{2\pi\omega} \right)^{\frac{1}{2}}. \tag{2.18}$$

The evanescent surface wave travels in towards the edge where it is evidently ‘scattered’ into a radially outgoing sound wave. There is a directional dependence in the amplitude in the form of a ‘Doppler’ factor $1/(1 - m \cos \theta)$. The waves are beamed most strongly in the forward direction as seen in figure 2. The beaming effect becomes more pronounced as the surface wave speed approaches that of sound.

2.2. The energetics of the motion

The question now arises as to how much energy is radiated from the surface. This can be calculated by evaluating the intensity I on the surface, where I is the product of the pressure and the normal velocity.

The pressure on the surface for $x < 0$ is taken from (2.6), and after some rearrangement the time-averaged surface intensity is then

$$\begin{aligned} \bar{I} &= \frac{1}{2} \text{Re} (p(x, 0, t) v_n^*) \\ &= -\frac{1}{4} \rho_0 v^2 c \frac{\partial}{\partial m'} \int_{-\infty}^{(\omega/c)x} \{ \sin m' \xi J_0(\xi) - \cos m' \xi N_0(\xi) \} \frac{d\xi}{\xi}, \end{aligned} \tag{2.19}$$

where $\xi = m\zeta$, $m' = 1/m$, and J_0 and N_0 are zero-order Bessel functions of the first and second kind.

To find the total rate Φ at which energy is radiated from the boundary requires that \bar{I} be integrated with respect to x over the region $x < 0$.

Thus

$$\Phi = -\frac{1}{4} \rho_0 v^2 c \frac{\partial}{\partial m'} \int_{-\infty}^0 dx \int_{-\infty}^{(\omega/c)x} \{ \sin m' \xi J_0(\xi) - \cos m' \xi N_0(\xi) \} \frac{d\xi}{\xi}. \tag{2.20}$$

Changing the order of integration and integrating with respect to x gives

$$\begin{aligned} \Phi &= -\frac{\rho_0 v^2 c^2}{4\omega} \frac{\partial}{\partial m'} \int_0^\infty \{ \sin m' \xi J_0(\xi) + \cos m' \xi N_0(\xi) \} d\xi \\ &= 0, \end{aligned} \tag{2.21}$$

when $m' > 1$. This means that there is *no* energy radiated through the boundary at $y = 0$.

In the far field, however, the cylindrical sound wave

$$p_r = \frac{A}{r^{\frac{1}{2}}} \frac{1}{1 - m \cos \theta} i e^{i\omega(t-r/c)} e^{i\frac{1}{2}\pi} \quad (2.22)$$

has radial intensity

$$I_r = \frac{1}{2\rho_0 c} \operatorname{Re}(p_r p_r^*). \quad (2.23)$$

The time-averaged rate at which energy flows away in the sound wave is therefore

$$\begin{aligned} \Phi_r &= \int_0^\pi \bar{I}_r d\theta = \frac{A^2}{2\rho_0 c} \int_0^\pi \frac{d\theta}{(1 - m \cos \theta)^2} \\ &= \frac{\rho_0 v^2}{4k} \frac{1}{(1 - m^2)^{\frac{3}{2}}} \frac{\omega}{k}, \end{aligned} \quad (2.24)$$

most of it going downstream because of the beaming effect emphasized in figure 2.

We have now ascertained that there is energy travelling outwards in the sound wave, and that its source is not in the surface $y = 0$.

Now we consider the energy approaching from infinity in the evanescent wave $E(x, t)$.

The x -velocity of the fluid elements above the surface is

$$v_x = \frac{v}{(1 - m^2)^{\frac{1}{2}}} i e^{i(\omega t - kx)} e^{-ky(1 - m^2)^{\frac{1}{2}}}. \quad (2.25)$$

The rate at which energy fluxes in towards the edge in the evanescent field Φ_e , can thus be found by integrating over a vertical control surface.

Consequently

$$\Phi_e = \frac{1}{2} \int_0^\infty \operatorname{Re}(E v_x^*) dy = \frac{\rho_0 v^2}{4k} \frac{1}{(1 - m^2)^{\frac{3}{2}}} \frac{\omega}{k}. \quad (2.26)$$

By noting that (2.24), the energy in the cylindrical wave, and (2.26), that incoming along the boundary $y = 0$ with the surface wave, are equal, the energy balance in the system is apparent. The energy in the evanescent wave approaching the edge is totally transferred into the cylindrical wave; the surface does no work. (In our model the surface is capable of producing or absorbing an infinite amount of energy.)

2.3. Conservation of momentum

Each unit area of a deformed surface as shown in figure 3 will experience a form drag $d_f = p_s(\partial\xi/\partial x)$ in the positive x -direction.

The total x -direction force on the surface is

$$D_f = \int_{y=\xi(x,t)} p(x, \xi(x, t), t) \delta_{jx} dS_j. \quad (2.27)$$

To second order in $k\xi_0$, since

$$p(x, \xi(x, t), t) = p(x, 0, t) + \frac{\partial p}{\partial y}(x, 0, t) \xi(x, t) + O(k^2 \xi_0^2), \quad (2.28)$$

$$D_f = \int_{y=0} p(x, 0, t) \frac{\partial \xi}{\partial x} dx. \quad (2.29)$$

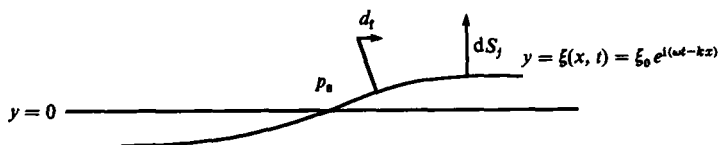


FIGURE 3. The forces acting on the deformed surface.

Now
$$\xi(x, t) = -i \frac{v}{\omega} H(-x) e^{i(\omega t - kx)}, \quad (2.30)$$

so that the boundary slope is

$$\frac{\partial \xi}{\partial x} = -\frac{k}{\omega} v_n + i \frac{v}{\omega} e^{i\omega t} \delta(x), \quad (2.31)$$

Taking the pressure p on the surface from (2.4)

$$\frac{1}{2} \operatorname{Re} \left(p \frac{\partial \xi^*}{\partial x} \right) = -\frac{k}{2\omega} \operatorname{Re} (p v_n^*) - \frac{v}{2\omega} \delta(x) \operatorname{Re} (ip e^{-i\omega t}). \quad (2.32)$$

Integrating over x gives the total force D_t on the surface due to the form drag as

$$D_t = -\frac{v}{2\omega} \int_{-\infty}^{\infty} \delta(x) \operatorname{Re} (ip e^{-i\omega t}) dx, \quad (2.33)$$

because
$$\int_{-\infty}^{\infty} \operatorname{Re} (p v_n^*) dx = \Phi = 0,$$

from (2.21). Hence

$$\begin{aligned} D_t &= \frac{1}{4} \rho_0 v^2 \int_{-\infty}^{\infty} \delta(x) dx \int_x^{\infty} \left\{ \sin k\eta J_0 \left(\frac{\omega}{c} \eta \right) - \cos k\eta N_0 \left(\frac{\omega}{c} \eta \right) \right\} d\eta \\ &= \frac{1}{4} \rho_0 v^2 \int_0^{\infty} \left\{ \sin k\eta J_0 \left(\frac{\omega}{c} \eta \right) - \cos k\eta N_0 \left(\frac{\omega}{c} \eta \right) \right\} d\eta \\ &= \frac{\rho_0 v^2}{2k} \frac{1}{(1-m^2)^{\frac{1}{2}}}. \end{aligned} \quad (2.34)$$

The force which the surface exerts on the fluid evidently acts in the negative x -direction, i.e. against the incoming evanescent wave. Since the fluid is in steady periodic motion this mean force must be balanced by other forces; i.e. the pressure and Reynolds' stress acting on the distant control surface.

First consider the cylindrical wave p_r as defined by (2.22), and take the control surface to be a large semicircle centred on $x = y = 0$. The time-averaged force P_r exerted on the contained fluid in the negative x -direction due to the departing wave is

$$P_r = \overline{\int_0^{\pi-\epsilon} (p_r \cos \theta + \rho v_{xr} v_r) r d\theta}, \quad (2.35)$$

where $\epsilon = \sin^{-1}(\xi(x, t)/r)$, and v_{xr} is the x -component of the radial velocity v_r . (The overbar denotes the time average of the real part of the quantity, or in the case of a product the time average of the product of the real parts.)

Then

$$P_r = \int_0^{\pi} \overline{p_r + \rho v_r^2} \cos \theta r d\theta - \int_0^{\epsilon} (p_r + \rho v_r^2) \cos \theta r d\theta. \quad (2.36)$$

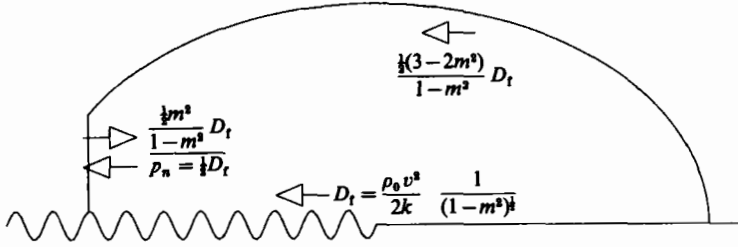


FIGURE 4. The control surface, with the forces acting on the fluid inside from each part of the system. p_n is the force induced by the second-order pressure defined in (2.40).

To second order in $k\xi_0$, and as $r \rightarrow \infty$, since $v_r = p_r/\rho_0 c$,

$$P_r = \rho_0 \int_0^\pi v_r^2 \cos \theta r d\theta = \frac{\rho_0 v^2}{4k} \frac{m^2}{(1-m^2)^{3/2}}. \quad (2.37)$$

The force P_e on the left-hand side of the volume due to the incoming evanescent wave E can now be found by considering the control surface to be vertical and positioned sufficiently far to the left that this wave is the only important disturbance. Then

$$\begin{aligned} P_e &= \int_{\xi(x,t)}^{\infty} (E + \rho v_x^2) dy \\ &= \int_0^\infty (\bar{E} + \overline{\rho v_x^2}) dy - \int_0^{\xi(x,t)} (E + \rho v_x^2) dy. \end{aligned} \quad (2.38)$$

The pressure field as obtained from (2.1) is correct up to order $k\xi_0$, but on any distant control surface the pressure field will be required to second order. This second-order pressure p_2 is (King 1934)

$$p_2 = \frac{1}{2\rho_0 c^2} P_1^2 - \frac{1}{2} \rho_0 v_1^2, \quad (2.39)$$

p_1 , and v_1 , being the first-order pressure and velocity respectively.

For a plane sound wave, since there is an equipartition between the kinetic and potential energy, $\bar{p}_2 = 0$. This is not so however for the incoming evanescent wave represented by (2.5), in which

$$\bar{p}_2 = -\frac{1}{2} \rho_0 v^2 e^{-2ky(1-m^2)^{1/2}}. \quad (2.40)$$

The first integral of (2.38) can be evaluated as

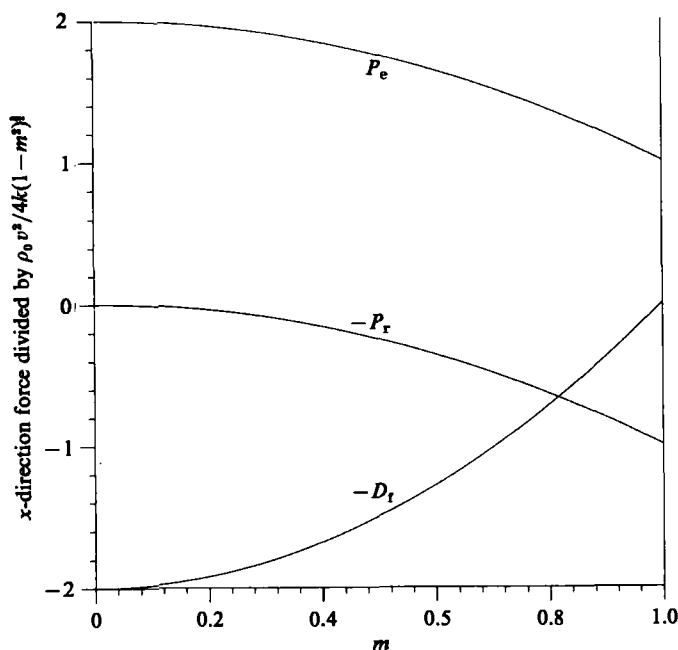
$$\frac{\rho_0 v^2}{4k} \frac{m^2}{(1-m^2)^{3/2}}, \quad (2.41)$$

while, to second order, the second integral is

$$\frac{1}{2} \operatorname{Re} (E(x, 0, t) \xi(x, t)^*) = -\frac{\rho_0 v^2}{2k} \frac{1}{(1-m^2)^{1/2}}. \quad (2.42)$$

Then from (2.41), and (2.42)

$$P_e = \frac{\rho_0 v^2}{4k} \frac{(2-m^2)}{(1-m^2)^{3/2}}. \quad (2.43)$$


 FIGURE 5. The components of the x -wise force on the control surface.

This is a force acting to the right on the control volume due to the presence of the evanescent field, and of course all of the forces balance in the equilibrium condition

$$P_e - P_r - D_t = 0. \quad (2.44)$$

As we have seen, the non-zero mean value of the pressure perturbation is crucial to this balance. This is shown diagrammatically in figure (4), and quantitatively in figure 5.

3. A surface wave moving away from an edge

3.1. The pressure field

For this case we specify a normal velocity

$$v'_n = vH(x) e^{i(\omega t - kx)}, \quad (3.1)$$

on $y = 0$. The pressure field that this implies can be found from the earlier results. By noting that $v_n + v'_n$ produces the evanescent field E , it is clear that v'_n produces the field $p' = E - p$, where p is (2.4).

Then

$$p' = \frac{1}{2}\rho_0 v\omega \int_0^\infty e^{i(\omega t - kx')} H_0^{(2)}\left(\frac{\omega}{c}((x-x')^2 + y^2)^{1/2}\right) dx', \quad (3.2)$$

and the asymptotic form is

$$p' \sim H(x) E(x, t) - \frac{A}{r^{1/2}} \frac{1}{1 - m \cos \theta} i e^{i\omega(t-r/c)} e^{i\frac{1}{4}\pi}. \quad (3.3)$$

3.2. *The energetics of the motion*

When a surface wave moves away from an edge there is an evanescent wave in the fluid together with a cylindrical sound wave. They carry energy away, each at a rate

$$\frac{\rho_0 v^2}{4k} \frac{1}{(1-m^2)^{\frac{3}{2}}} \frac{\omega}{k} \quad (3.4)$$

as calculated in (2.24), and (2.26).

It is clear that the transfer of energy which took place between these two waves in the previous situation no longer occurs. The surface must now do work on the fluid; a fact which can be verified by following a similar argument to that of §2.2.

In this case

$$\bar{I} = -\frac{1}{4}\rho_0 v^2 \frac{\omega}{k} \int_{kx}^{\infty} (\cos \zeta J_0(m\zeta) + \sin \zeta N_0(m\zeta)) d\zeta, \quad (3.5)$$

for $x > 0$. Then

$$\bar{I} = -\frac{1}{4}\rho_0 v^2 c \frac{\partial}{\partial m'} \int_{(\omega/c)x}^{\infty} (\sin m' \xi J_0(\xi) - \cos m' \xi N_0(\xi)) \frac{d\xi}{\xi}. \quad (3.6)$$

The rate at which energy is radiated from the whole surface is then

$$\begin{aligned} \Phi' &= \int_0^{\infty} \bar{I} dx = -\frac{\rho_0 v^2 c^2}{4\omega} \frac{\partial}{\partial m'} \int_0^{\infty} (\sin m' \xi J_0(\xi) - \cos m' \xi N_0(\xi)) d\xi \\ &= \frac{\rho_0 v^2}{2k} \frac{1}{(1-m^2)^{\frac{3}{2}}} \frac{\omega}{k}, \end{aligned} \quad (3.7)$$

which is the sum of that radiated in the evanescent and sound waves. The surface supplies energy at a sufficient rate to support both the sound and evanescent waves.

3.3. *Conservation of momentum*

As in §2.3 the forces within the system must balance, with the evanescent wave and the cylindrical wave still inducing forces of the same magnitude on the control volume, which is now chosen as shown in figure 6. The force which is associated with the evanescent wave now acts in the opposite direction, because the wave is leaving rather than entering the control volume.

The drag on the surface still has to be evaluated directly using (3.2). The displacement is now

$$\xi(x, t) = -i \frac{v}{\omega} H(x) e^{i(\omega t - kx)}, \quad (3.8)$$

so that

$$\frac{\partial \xi}{\partial x} = -\frac{k}{\omega} v'_n - i \frac{v}{\omega} e^{i\omega t} \delta(x). \quad (3.9)$$

The drag,

$$\begin{aligned} D'_t &= -\frac{k}{2\omega} \int_{y=0} \operatorname{Re}(p' v'_n^*) dS + \frac{v}{2\omega} \int_s p \delta(x) \operatorname{Re}(ip' e^{-i\omega t}) dS \\ &= -\frac{k}{\omega} \Phi' + \frac{v}{2\omega} \operatorname{Re}(ip' e^{-i\omega t})|_{x=0}, \end{aligned} \quad (3.10)$$

where Φ' is defined by (3.7), and p' by (3.2).

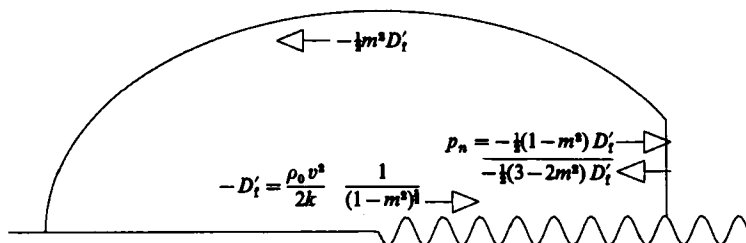


FIGURE 6. The control surface with the forces acting on the fluid inside from each part of the system. p_n is the force induced by the second-order pressure defined in (2.40).

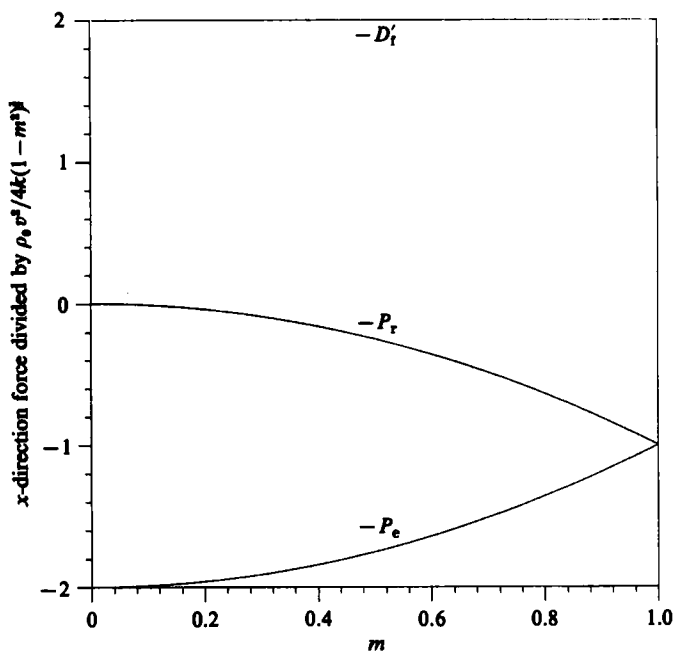


FIGURE 7. The components of the x -wise force on the control surface.

Then

$$\begin{aligned} \frac{v}{2\omega} \operatorname{Re} (ip' e^{-i\omega t})|_{x=0} &= -\frac{1}{4}\rho_0 v^2 \int_{-\infty}^0 \left\{ \sin k\eta J_0\left(\frac{\omega}{c}\eta\right) - \cos k\eta N_0\left(\frac{\omega}{c}\eta\right) \right\} d\eta \\ &= 0, \end{aligned} \quad (3.11)$$

giving

$$D'_t = -\frac{\rho_0 v^2}{2k} \frac{1}{(1 - m^2)^{1/2}}. \quad (3.12)$$

This force exerted by the surface on the fluid acts in the positive x -direction, i.e. it acts in the direction of the departing evanescent wave.

The balance

$$P_r + P_e + D'_t = 0, \quad (3.13)$$

is qualitatively shown in figure 6, and quantitatively in figure 7.

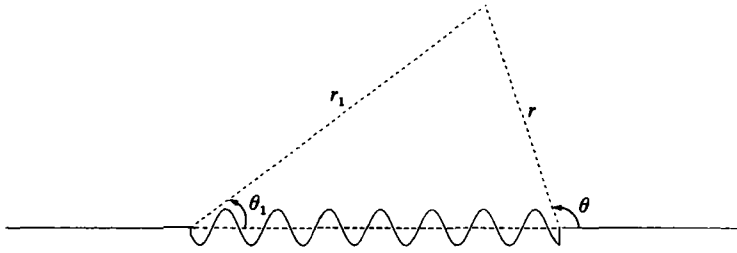


FIGURE 8. The coordinate system for equation (4.3).

4. A surface wave crossing a strip

4.1. *The pressure field*

Now we consider the situation where the surface motion is confined to the region $-a \leq x \leq 0$, where the normal velocity v''_n is specified by

$$v''_n = v(H(-x) - H(-x-a)) e^{i(\omega t - kx)}. \tag{4.1}$$

The response is expressible as a superposition of the two fields already considered. We find that the pressure field p'' due to (4.1) is

$$p'' = \frac{1}{2} \rho_0 v \omega \int_{-a}^0 e^{i(\omega t - kx')} H_0^{(2)} \left(\frac{\omega}{c} ((x-x')^2 + y^2)^{\frac{1}{2}} \right) dx', \tag{4.2}$$

the asymptotic form being

$$p'' \underset{r \rightarrow \infty}{\sim} (H(-x) - H(-x-a)) p_e(x, t) + \frac{A}{r^{\frac{1}{2}} 1 - m \cos \theta} i e^{i\omega(t-r/c)} e^{i\frac{1}{4}\pi} - \frac{A}{r^{\frac{1}{2}} 1 - m \cos \theta_1} i e^{i\omega(t-r/c)} e^{i(\frac{1}{4}\pi + ka)}, \tag{4.3}$$

where A is given by (2.18) and

$$r_1 = (r^2 + a^2 + 2ar \cos \theta)^{\frac{1}{2}}, \tag{4.4}$$

$$\cos \theta_1 = \frac{a + r \cos \theta}{(r^2 + a^2 + 2ar \cos \theta)^{\frac{1}{2}}}. \tag{4.5}$$

The coordinate system is shown in figure 8.

4.2. *The energetics of the motion*

For $-a < x < 0$ the normal surface velocity is given by

$$v e^{i(\omega t - kx)}, \tag{4.6}$$

and the time-averaged intensity on the surface is

$$\frac{1}{2} \text{Re} (p'' v e^{-i(\omega t - kx)}) = \frac{1}{4} \rho_0 v^2 \omega \int_x^{x+a} \left\{ \cos k\eta J_0 \left(\frac{\omega}{c} \eta \right) + \sin k\eta N_0 \left(\frac{\omega}{c} \eta \right) \right\} d\eta, \tag{4.7}$$

which gives the total power output of the surface as

$$\begin{aligned}
 \Phi_s &= \frac{1}{4} \rho_0 v^2 \omega \int_{-a}^0 dx \int_x^{x+a} \left\{ \cos k\eta J_0\left(\frac{\omega}{c}\eta\right) + \sin k\eta N_0\left(\frac{\omega}{c}\eta\right) \right\} d\eta \\
 &= \frac{1}{4} \rho_0 v^2 \omega \int_{-a}^0 \left\{ \cos k\eta J_0\left(\frac{\omega}{c}\eta\right) + \sin k\eta N_0\left(\frac{\omega}{c}\eta\right) \right\} (\eta+a) d\eta \\
 &\quad + \frac{1}{4} \rho_0 v^2 \omega \int_0^a \left\{ \cos k\eta J_0\left(\frac{\omega}{c}\eta\right) + \sin k\eta N_0\left(\frac{\omega}{c}\eta\right) \right\} (a-\eta) d\eta \\
 &= \frac{\rho_0 v^2 \omega}{2k} \int_0^{ka} \cos \xi J_0(m\xi) (ka - \xi) d\xi.
 \end{aligned} \tag{4.8}$$

When $r \gg a$,

$$r_1 \sim r + a \cos \theta, \quad \cos \theta \sim \cos \theta_1. \tag{4.9}$$

and the far-field pressure can be written as

$$p_{\text{far}}'' = \frac{A}{r^{\frac{1}{2}}} \frac{1}{1-m \cos \theta} \{ e^{i\omega(t-r/c)} e^{i\frac{1}{2}\pi} - e^{i\omega(t-r/c)} e^{i\frac{1}{2}\pi} e^{ika(1-m \cos \theta)} \}. \tag{4.10}$$

This field has intensity

$$\bar{I} = \frac{\overline{p_{\text{far}}''^2}}{\rho_0 c} = \frac{A^2}{\rho_0 c r} \frac{1}{(1-m \cos \theta)^2} (1 - \cos(ka(1-m \cos \theta))), \tag{4.11}$$

so that the total power radiated outwards to infinity is

$$\Phi_r = \int_0^\pi \bar{I} r d\theta = \frac{\rho_0 v^2 \omega}{2k^2 \pi} \int_0^\pi \frac{(1 - \cos(ka(1-m \cos \theta)))}{(1-m \cos \theta)^2} d\theta. \tag{4.12}$$

The equivalence of Φ_s , and Φ_r can be verified by replacing $J_0(m\xi)$ in (4.8), using the identity;

$$J_0(m\xi) = \frac{1}{\pi} \int_0^\pi \cos(m\xi \cos \theta) d\theta. \tag{4.13}$$

Then

$$\begin{aligned}
 \Phi_s &= \frac{\rho_0 v^2 \omega}{2k^2 \pi} \int_0^{ka} \cos \xi (ka - \xi) d\xi \int_0^\pi \cos(m\xi \cos \theta) d\theta \\
 &= \frac{\rho_0 v^2 \omega}{4k^2 \pi} \int_0^\pi d\theta \int_0^{ka} (ka - \xi) (\cos \xi (1 + m \cos \theta) + \cos \xi (1 - m \cos \theta)) d\xi \\
 &= \frac{\rho_0 v^2 \omega}{4k^2 \pi} \int_0^\pi d\theta \left\{ \frac{(1 - \cos(ka(1-m \cos \theta)))}{(1+m \cos \theta)^2} + \frac{(1 - \cos(ka(1-m \cos \theta)))}{(1-m \cos \theta)^2} \right\} \\
 &= \frac{\rho_0 v^2 \omega}{2k^2 \pi} \int_0^\pi \frac{(1 - \cos(ka(1-m \cos \theta)))}{(1-m \cos \theta)^2} d\theta \\
 &= \Phi_r.
 \end{aligned} \tag{4.14}$$

The asymptotic form as m tends to zero is independent of m as can be seen from (4.8) with $J_0(m\xi)$ set equal to unity:

$$\Phi_s \underset{m \rightarrow 0}{\sim} \frac{\rho_0 v^2 \omega}{2k^2} (1 - \cos ka). \tag{4.15}$$

When ka is small (4.12) is the more useful expression.

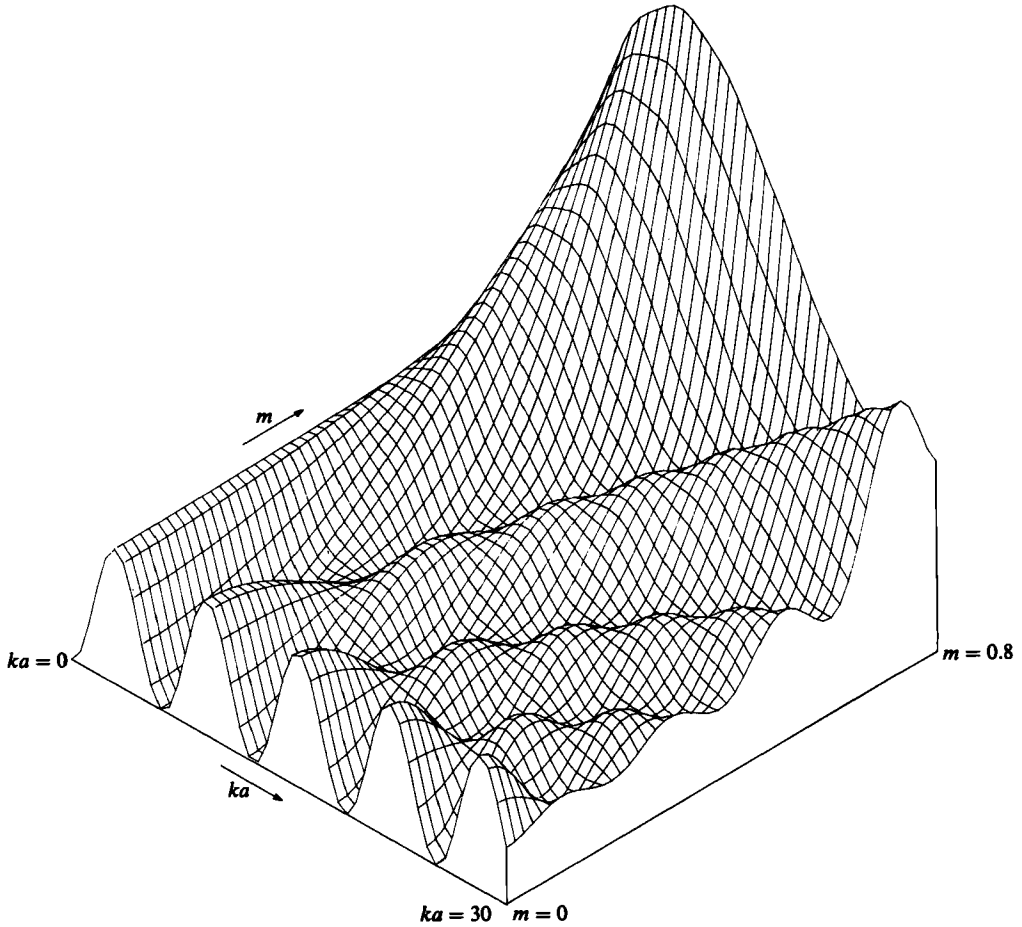


FIGURE 9. A representation of the energy radiated by the strip as a function of both Mach number m , and ka .

Using the fact that

$$(1 - \cos(ka(1 - m \cos \theta))) = - \sum_{n=1}^{\infty} \frac{(-1)^n}{(2n)!} (ka)^{2n} (1 - m \cos \theta)^{2n}, \quad (4.16)$$

$$\Phi_s = - \frac{\rho_0 v^2 \omega}{2k^2 \pi} \sum_{n=1}^{\infty} \frac{(-1)^n}{(2n)!} (ka)^{2n} \int_0^\pi (1 - m \cos \theta)^{2n-2} d\theta. \quad (4.17)$$

Gradshteyn & Ryzhik (1980, p. 382, §3.661(3)), give the identity

$$\int_0^\pi (1 - m \cos \theta)^{2n-2} d\theta = \pi(1 - m^2)^{n-1} P_{2n-2} \left(\frac{1}{(1 - m^2)^{\frac{1}{2}}} \right), \quad (4.18)$$

where P_n are Legendre's Polynomials, so that to order $(ka)^2$

$$\Phi_s = \frac{\rho_0 v^2 \omega}{4k^2} (ka)^2, \quad (4.19)$$

an expression that is also independent of m and the fluid's compressibility.

To find a form for Φ_s in the limit as $ka \rightarrow \infty$ the following integrals must be considered for large values of ka :

$$I_1 = \int_0^{ka} \cos \xi J_0(m\xi) d\xi, \quad (4.20)$$

$$I_2 = \int_0^{ka} \xi \cos \xi J_0(m\xi) d\xi. \quad (4.21)$$

These limits can be found simply by integration by parts, and the results are quoted from Levine (1980):

$$I_1 = - \int_{ka}^{\infty} \cos \xi J_0(m\xi) d\xi = - \frac{1}{m} \int_{(\omega/c)a}^{\infty} \cos\left(\frac{\eta}{m}\right) J_0(\eta) d\eta \\ \sim_{ka \rightarrow \infty} \frac{1}{1-m^2} J_0\left(\frac{\omega}{c}a\right) \sin ka - \frac{m}{1-m^2} J_1\left(\frac{\omega}{c}a\right) \cos ka; \quad (4.22)$$

$$I_2 \sim_{ka \rightarrow \infty} -\frac{1}{(1-m^2)^{\frac{3}{2}}} + J_1\left(\frac{\omega}{c}a\right) \left\{ -\frac{kam}{1-m^2} \cos ka + \frac{2m}{(1-m^2)^2} \sin ka \right\} \\ + J_0\left(\frac{\omega}{c}a\right) \left\{ \frac{(1+m^2)}{(1-m^2)^2} \cos ka + \frac{ka}{(1-m^2)} \sin ka \right\}. \quad (4.23)$$

These asymptotic forms give

$$\Phi_s \sim_{ka \rightarrow \infty} \frac{\rho_0 v^2 \omega}{2k^2} (kaI_1 - I_2) \\ = \frac{\rho_0 v^2 \omega}{2k^2} \frac{1}{(1-m^2)^{\frac{3}{2}}} - \frac{\rho_0 v^2 \omega}{k^2} \frac{1}{(1-m^2)^2} J_1\left(\frac{\omega}{c}a\right) m \sin ka \\ - \frac{\rho_0 v^2 \omega}{2k^2} \frac{(1+m^2)}{(1-m^2)^2} J_0\left(\frac{\omega}{c}a\right) \cos ka. \quad (4.24)$$

As $(\omega/c)a \rightarrow \infty$,

$$\Phi_s \rightarrow \frac{\rho_0 v^2 \omega}{2k^2} \frac{1}{(1-m^2)^{\frac{3}{2}}}.$$

This is actually the energy generated by the two wave 'ends' acting independently, each of which, we have shown already, generates an acoustic power,

$$\frac{\rho_0 v^2 \omega}{4k^2} \frac{1}{(1-m^2)^{\frac{3}{2}}}, \quad (4.25)$$

as found in the analysis of §§2.2 and 3.2. The dependence of the energy on ka , and m , is shown in figure 9.

4.3. Conservation of momentum

The drag on the surface can be evaluated in a similar manner to §§2.3 and 3.3. In this case

$$\frac{\partial \xi}{\partial x} = -\frac{k}{\omega} v_n'' + i \frac{v}{\omega} e^{i(\omega t - kx)} (\delta(x) - \delta(x+a)), \quad (4.26)$$

and the drag force over the whole surface is

$$\begin{aligned} D_f'' &= -\frac{k}{\omega} \Phi_s + \frac{v}{\omega} \int_{-\infty}^{\infty} \operatorname{Re} (ip'' e^{-i(\omega t - kx)}) (\delta(x) + \delta(x+a)) dx \\ &= -\frac{k}{\omega} \Phi_s + \frac{\rho_0 v^2}{2k} \int_0^{ka} \sin \xi J_0(m\xi) d\xi. \end{aligned} \quad (4.27)$$

Integration by parts of expression (4.8) for Φ_s , and its substitution into (4.27) gives

$$D_f'' = -\frac{\rho_0 v^2 m}{2k} \int_0^{ka} \sin \xi (ka - \xi) J_1(m\xi) d\xi. \quad (4.28)$$

The rate at which the x -momentum is convected out through a distant surface is

$$\begin{aligned} P &= \int_s \rho_0 \overline{v_x v_r} dS \\ &= \frac{\rho_0 v^2 m}{2k\pi} \int_0^\pi \frac{\cos \theta}{(1 - m \cos \theta)^2} (1 - \cos(ka(1 - m \cos \theta))) d\theta. \end{aligned} \quad (4.29)$$

In this case the momentum in the distant sound field is equal to the surface drag, i.e.

$$P + D_f'' = 0. \quad (4.30)$$

The equality can be established by noting that

$$\int_0^{ka} \sin \xi J_0(m\xi) d\xi = \frac{1}{\pi} \int_0^\pi \frac{(1 - \cos(ka(1 - m \cos \theta)))}{(1 - m \cos \theta)} d\theta, \quad (4.31)$$

and by substituting this into (4.27) with expression (4.12) for Φ_s .

By expanding $J_1(m\xi)$ for small argument we obtain an expression for D_f'' as m tends to zero:

$$\begin{aligned} D_f'' &= -\frac{\rho_0 v^2}{2k} \int_0^{ka} \sin \xi (ka - \xi) \left(\frac{1}{2} m \xi + O(m^2 \xi^2) \right) d\xi \\ &\underset{m \rightarrow 0}{\sim} -\frac{\rho_0 v^2 m^2}{2k} \left\{ 1 - \cos ka - \frac{1}{2} ka \sin ka \right\}. \end{aligned} \quad (4.32)$$

The surface drag is essentially due to the fluid's compressibility and originates in the fore and aft beams of the sound wave caused by convective source motion.

To find an expression for D_f'' when ka is small, (4.29) is used: $1 - \cos(ka(1 - m \cos \theta))$ is expanded as a power series in $ka(1 - m \cos \theta)$, to give

$$D_f'' = \frac{\rho_0 v^2 m}{2k\pi} \sum_{n=1}^{\infty} \frac{(-1)^n}{(2n)!} (ka)^{2n} I_n, \quad (4.33)$$

where

$$\begin{aligned} I_r &= \int_0^\pi \cos \theta (1 - m \cos \theta)^{2r-2} d\theta \\ &= -\frac{\pi}{m} \left\{ (1 - m^2)^{n-\frac{1}{2}} P_{2n-1} \left(\frac{1}{(1 - m^2)^{\frac{1}{2}}} \right) - (1 - m^2)^{n-1} P_{2n-2} \left(\frac{1}{(1 - m^2)^{\frac{1}{2}}} \right) \right\}. \end{aligned} \quad (4.34)$$

$I_1 = 0$, so that the lowest-order terms are $(ka)^4$. To fourth order in ka therefore

$$\begin{aligned} D_f'' &= \frac{\rho_0 v^2 m}{2k\pi} \frac{1}{4!} (ka)^4 I_2 \\ &= -\frac{1}{48} \frac{\rho_0 v^2}{k} m^2 (ka)^4. \end{aligned} \quad (4.35)$$

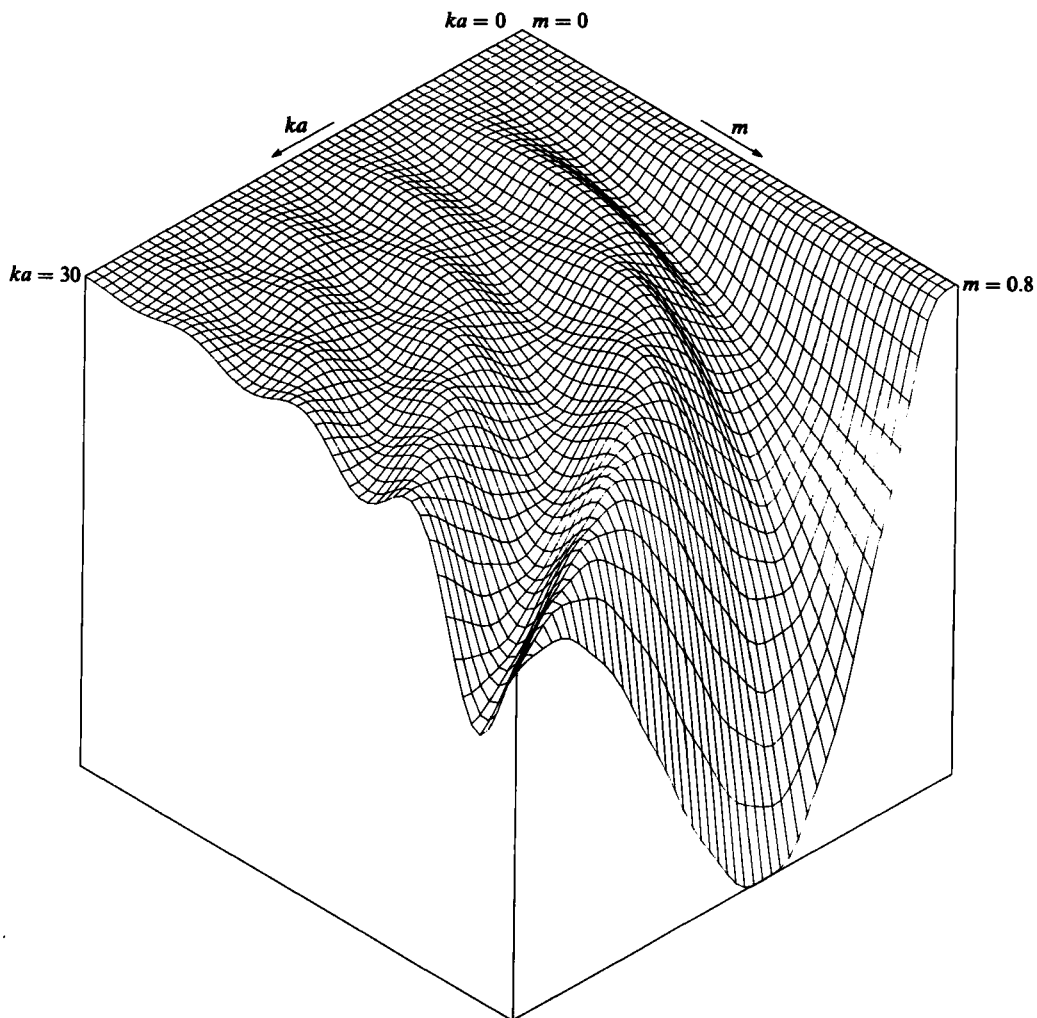


FIGURE 10. A representation of the drag on the surface as a function of both the Mach number m , and ka .

When ka is very large, the asymptotic form of Φ_s is given by (4.24), which can be placed in (4.27) along with the approximation

$$\int_0^{ka} \sin \xi J_0(m\xi) d\xi \underset{ka \rightarrow \infty}{\sim} \frac{1}{(1-m^2)^{\frac{1}{2}}} - \frac{1}{1-m^2} J_0\left(\frac{\omega}{c}a\right) \cos ka - \frac{m}{1-m^2} J_1\left(\frac{\omega}{c}a\right) \sin ka. \quad (4.36)$$

Then

$$D_1'' \underset{ka \rightarrow \infty}{\sim} \frac{\rho_0 v^2}{2k} \frac{1}{(1-m^2)^{\frac{1}{2}}} - \frac{\rho_0 v^2}{2k} \frac{1}{(1-m^2)^{\frac{1}{2}}} + \frac{\rho_0 v^2}{2k} \frac{m(1+m^2)}{(1-m^2)^2} J_1\left(\frac{\omega}{c}a\right) \sin ka + \frac{\rho_0 v^2}{2k} \frac{2m^2}{(1-m^2)^2} J_0\left(\frac{\omega}{c}a\right) \cos ka. \quad (4.37)$$

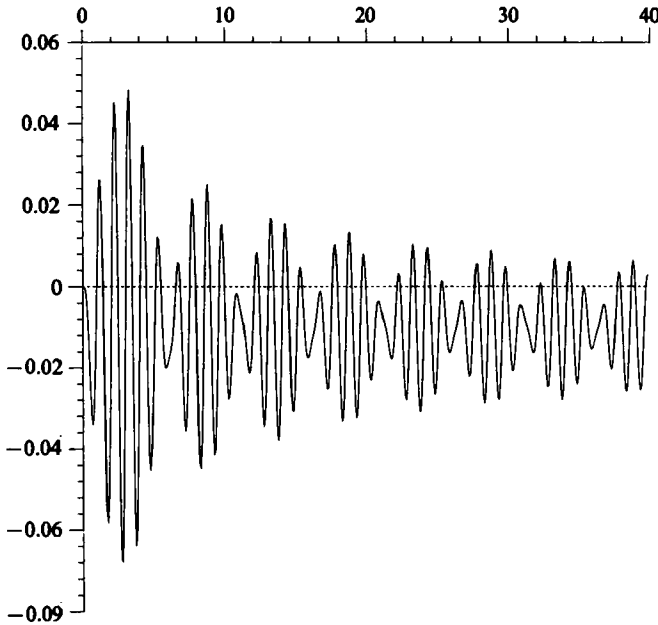


FIGURE 11. This shows the drag on the surface (normalized by $\rho_0 v^2/2k$) for $m = 0.1$ as a function of the number of wavelengths present in the strip.

As $(\omega/c)a = mka \rightarrow \infty$, D_f'' tends to

$$-\frac{\rho_0 v^2}{2k} \frac{m^2}{(1-m^2)^{\frac{3}{2}}}, \quad (4.38)$$

which is the sum of the drag forces on two independent wave 'ends', found in §§2.3 and 3.3. Figure 10 shows the drag on the surface as a function of ka and m .

As the strip becomes very wide the interaction between the ends becomes less, until eventually in the limit as ka becomes much larger than $1/m$ they are no longer coupled, and behave independently.

It is interesting to note that the drag on the surface can act both in the same direction, and the opposite direction to that in which the surface wave is travelling. This effect occurs only at small Mach numbers and the thrust is seen as a positive drag force in figure 11. From (4.32), which applies for small values of m , the condition for no drag can be shown to be

$$\tan \frac{1}{2}ka = \frac{1}{2}ka, \quad \text{or } ka = 2n\pi, \quad n \text{ an integer.} \quad (4.39)$$

From (4.15), when $ka = 2n\pi$, then $\Phi_s = 0$ also. Thus at vanishing Mach number the surface motion radiates no energy, nor any momentum. Only a near-field disturbance is apparent.

5. The fluid-loaded membrane

The previous sections deal with the idealized model of a surface on which the motion is exactly prescribed. In real surface vibration problems there is a dependence of the surface motion on the sound field, and this complicates the analysis considerably, especially when there is an edge present. Davies (1974) studied the motion of

a semi-infinite fluid-loaded membrane, and an asymptotic form of his results can be obtained directly from our analysis.

Davies considered a membrane under tension lying in the region $x < 0$, the end of the membrane being fixed at $x = 0$, with a rigid baffle in the region $x > 0$. The membrane is fluid loaded, and Davies calculated the reflection coefficient of surface waves incident on the edge, and the sound energy radiated by the wave-edge interaction.

If the membrane is lightly loaded, and the wave speed for the unloaded membrane very slow, it can be expected that while there is some energy radiated as sound, it is insignificant when compared to the energy in the membrane itself. The wave reflected at the edge must therefore be equal and opposite to the incident wave. From the analysis of §§2 and 3 it can be shown by superimposing the incident and outgoing surface waves of equal amplitude that there is a cylindrical wave of twice the amplitude of (2.22) centred on the edge. This radiates energy to the far field at a rate

$$\frac{\rho_0 v^2 \omega}{k k}, \tag{5.1}$$

which is in agreement with Davies (§VI, (i)).

Again for a lightly fluid-loaded membrane, if the free membrane wave speed is highly supersonic, then the incident waves, in the fluid-loaded case, can be expected to be just subsonic. The actual speed can be found by considering the equation of motion for a fluid-loaded membrane

$$\sigma \frac{\partial^2 \xi}{\partial t^2} - T \frac{\partial^2 \xi}{\partial x^2} = -p(x, 0, t), \tag{5.2}$$

where $p(x, y, t)$ satisfies the wave equation, and there is the additional condition of continuity of displacement at the boundary between fluid and membrane.

The dispersion relation for a steady harmonic wave travelling on the boundary is

$$r^2 \gamma^3 - \gamma(1 - r^2) - \frac{1}{\mu} = 0, \tag{5.3}$$

where $\gamma = (1 - m^2)^{\frac{1}{2}}$, m being the phase speed on the membrane divided by the sound speed, $r = (T/\sigma c^2)^{\frac{1}{2}}$, the ratio of the free membrane wave speed to that of sound, and $\mu = \sigma\omega/\rho_0 c$ the fluid-loading parameter.

When $r^2 \gg 1$, and $\mu \gg 1$, then if $m \sim 1$, (5.3) can be approximated to give

$$\gamma = (1 - m^2)^{\frac{1}{2}} = \frac{1}{\mu r^2}, \tag{5.4}$$

which is a very small quantity, confirming that the speed of the surface wave is very close indeed to, but less than, that of sound.

A wave which is only just subsonic, and which is incident on an edge induces the beaming effect that we described in §2.1 (see figure 2). Very little of this energy is reflected and Davies (§VI, (iii)) calculates that the radiated power is then

$$\frac{\rho_0 v^2}{4k} \frac{1}{\gamma^3} \frac{\omega}{k}, \tag{5.5}$$

which agrees exactly with our result (2.26).

6. Conclusion

An evanescent surface wave transports energy along the surface. If the wave is incident on an edge, its energy is scattered into sound. In the far field the sound is a centred cylindrical wave, decaying as r^{-1} . Its amplitude has a directional dependence $(1 - m \cos \theta)^{-1}$, r and θ being the polar coordinates centred on the edge, and m being the ratio of the surface phase speed to the sound speed. All of the energy which is travelling in the evanescent wave is transferred to the cylindrical sound wave; the surface is purely passive and does no work on the fluid.

A mean force is exerted on the fluid by the surface, and acts in the direction opposite to that in which the evanescent wave is travelling. This force balances the acoustic Reynolds stress, and mean pressure gradient induced as a nonlinear consequence of the surface wave.

On the other hand if a subsonic surface wave is driven away from an edge, despite there being an evanescent wave, and a cylindrical wave as before, the energetics and the form drag take on a different character.

The same amount of energy is radiated as sound but in this case the surface does work on the fluid to provide the energy requirement of both the evanescent and the sound fields.

The surface now exerts a force in the same direction as the evanescent wave is moving, and as before this is balanced by forces arising in the radiation stress and mean pressure gradient.

These two problems are combined to describe a surface wave driven across a finite strip.

Figures 9 and 10 show the energy radiated, and the drag on the strip respectively. As the strip width tends to infinity the system becomes the simple superposition of the two earlier cases. When the strip is an integral number of wavelengths wide, and the Mach number is small, the energy radiated and the drag on the surface are both of order of the Mach number.

By using these basic ideas, the more complex problem of a semi-infinite fluid-loaded membrane can be understood in some limiting cases. First, if the speed of a wave on the unloaded membrane is very subsonic, then the energy in the surface near field is very small, while that in the surface is relatively large. Because the fluid loading is light, any wave travelling along the membrane, incident on the edge will be reflected with almost an equal and opposite amplitude. From the first two cases studied in this paper, the energy radiated by such a system is easily calculated as (5.1). Secondly, if the membrane 'in vacuo' free wave speed is highly supersonic then the fluid-loaded wave travels at a speed only just less than that of sound. The energy in the near field is consequently very large, and when it is incident on the edge, none of it is reflected back. Both these cases conform with the exact calculations of Davies (1974).

REFERENCES

- DAVIES, H. G. 1974 Natural motion of a fluid-loaded semi-infinite membrane. *J. Acoust. Soc. Am.* **55**, 213–219.
- GRADSHTEYN, I. S. & RYZHIK, I. M. 1980 *Table of Integrals, Series, and Products*. (Corrected and enlarged edition.) Academic.
- HILL, D. C. 1986 Starting mechanics of an evanescent wave field. *J. Fluid Mech.* **165**, 319–333.
- KING, L. V. 1934 On the acoustic radiation pressure on spheres. *Proc. R. Soc. Lond. A* **147**, 212.

- LEVINE, H. 1980 A note on sound radiation into a uniformly flowing medium. *J. Sound Vib.* **71**, 1–8.
- MÖHRING, W. 1982 Wave energy, wave momentum, and propagation of sound in flows. *Fortschritte der Akustik*, FASE/DAGA '82.
- TAYLOR, G. I. 1942 The motion of a body in water when subjected to a sudden impulse. *Scientific Papers of G. I. Taylor, Vol. 3. Aerodynamics and the Mechanics of Projectiles and Explosives* (ed. G. K. Batchelor), pp. 306–308. Cambridge University Press.